Carbohydrate Polymers 83 (2011) 608–615

Contents lists available at ScienceDirect

Carbohydrate Polymers

journal homepage: www.elsevier.com/locate/carbpol

Modification of surface properties of thin polysaccharide films by low-energy electron exposure

Alena Ryzhkova, Ute Jarzak, Andreas Schäfer, Marcus Bäumer, Petra Swiderek*

Universität Bremen, Institute for Applied and Physical Chemistry, Fachbereich 2 (Chemie/Biologie), Leobener Straße/NW 2, Postfach 330440, 28334 Bremen, Germany

ARTICLE INFO

Article history:
Received 17 May 2010
Received in revised form 2 August 2010
Accepted 12 August 2010
Available online 19 August 2010

Keywords:
Low-energy electrons
Amylose
Chitosan
Thin films
Wetting properties

ABSTRACT

The effect of low-energy electron irradiation on thin layers of two different polysaccharide materials, namely amylose and chitosan, has been investigated. Modification of the samples occurs at electron energies as low as 5 eV. In the case of amylose, a change in the wetting properties is observed upon exposure. Loss of oxygen from the hydroxyl groups and consequent formation of a hydrocarbon material is responsible for this effect as revealed by analysing the samples before and after electron exposure by means of reflection absorption infrared spectroscopy (RAIRS) and X-ray photoelectron spectroscopy (XPS). It is shown that the amide side groups in chitosan are more reactive than the hydroxyl groups and consequently dominate the modifications in this case. Additional experiments by high-resolution electron energy loss spectroscopy (HREELS) on thin condensed films of the model compound α-D-glucose show that facile oxidation of the saccharide occurs in the presence of O_2. Traces of O_2 as a residual gas can therefore be held responsible for the formation of carboxyl groups that are observed by RAIRS in samples of amylose after electron exposure.

1. Introduction

The modification of polysaccharides by radiation treatment receives considerable interest because it can provide access to a wide range of applications of these abundant natural materials (Hai, Diep, Nagasawa, Yoshii, & Kume, 2003; Huang, Peng, Zhai, Li, & Wie, 2007; Khan, Ahmad, & Kronfli, 2006; Long, Wu, & Chen, 2007; Sharpatyi, 2003; Zhai, Yoshii, & Fume, 2003). As a simple example, radiation-degraded chitosan has been suggested as plant growth promoter (Hai et al., 2003), but the same material may also serve as a medium for radiation-induced production of metal nanoparticles (Long et al., 2007). The mechanical strength of biodegradable plastics based on starch can be improved by high-energy electron irradiation (Zhai et al., 2003). Also, irradiation of polysaccharides can lead to cross-linked materials, some of which exhibiting antibacterial properties, that serve as biodegradable hydrogels with potential applications such as drug delivery systems or wound dressing (Pekel, Yoshii, Fume, & Güven, 2004; Yoshii et al., 2003; Zhao et al., 2003).

Structured hydrogel films have been produced by electrochemical deposition on patterned electrodes (Wu et al., 2005). In this respect, radiation processing using a focussed electron beam or a mask technique may be an interesting alternative as it could produce the same structures with less production steps. In a mask-based process, an unfocussed low-energy electron source can replace the high-energy beam (Eck et al., 2000). Due to the low penetration depth of low-energy electrons, this is particularly appropriate if only the modification of the surface properties of the material is desired. The chemical modification in the irradiated material, on the other hand, is expected to be similar because secondary electrons with low energies are also abundant as reactive species under exposure to high-energy radiation (Sim & White, 2005).

It was shown recently that saccharide monomers decompose easily under exposure to low-energy electrons (Baccarelli et al., 2007; Bald, Kopyra, & Illenberger, 2006; Ptasińska, Denifl, Scheier, & Märk, 2004; Sulzer et al., 2006). Low-energy electron irradiation should thus be an efficient tool for modifying polysaccharides. The previous studies on different monosaccharides that were performed in the gas phase (deoxyribose (Ptasińska et al., 2004), D-ribose (Baccarelli et al., 2007; Bald et al., 2006), fructose (Sulzer et al., 2006)) have revealed that electrons with energies near 0 eV induce efficient fragmentation of the molecules and additional reactions channels open at energies above 5 eV. This includes not only loss of water but also leads to complete decomposition of the ring structure. At the same time, the produced fragments can be selected by proper tuning of the electron energy (Ptasińska et al., 2004; Sulzer et al., 2006). In order to gain more control over the radiation-induced modifications in the related polysaccharides, it is thus worth exploring the use of low-energy electrons.

* Corresponding author. Tel.: +49 421 218 63200; fax: +49 421 218 63188.
E-mail address: swiderek@uni-bremen.de (P. Swiderek).

0144-8617/$ – see front matter © 2010 Elsevier Ltd. All rights reserved.
doi:10.1016/j.carbpol.2010.08.029

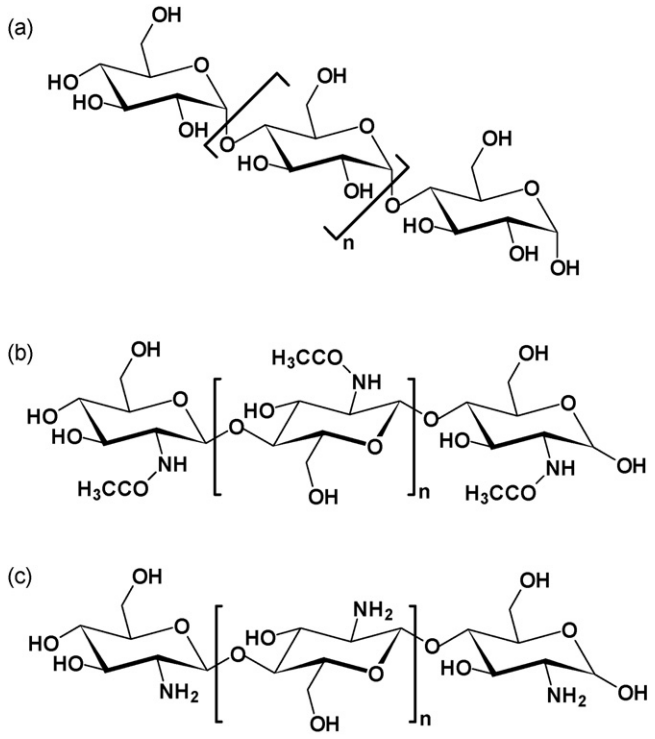

Fig. 1. Structure of the polysaccharides amylose (a), chitin (b), and a fully deacetylated chitosan (c). The chitosan used in the present study is partially deacetylated.

In this study the effect of low-energy electron irradiation on thin layers of two different polysaccharide materials, namely amylose and chitosan, the latter being the deacetylated or partially deacetylated form of chitin (Fig. 1), is investigated. In the case of amylose, an interesting change in the wetting properties is observed upon exposure. The chemical modifications underlying this effect are revealed by analysing the samples before and after electron exposure by means of reflection absorption infrared spectroscopy (RAIRS) and X-ray photoelectron spectroscopy (XPS). It is shown that the reactivity of the polysaccharide backbone is modified by the side groups present in a chitosan with some remaining degree of acetylation. In addition, to obtain insights into the effect of residual oxygen on the outcome of electron-induced reactions, an experiment is presented in which thin films of the monomer α-D-glucose before and after exposure to low-energy electrons in ultrahigh vacuum (UHV) and under a certain O_2 partial pressure are characterized using high-resolution electron energy loss spectroscopy (HREELS).

2. Experimental

2.1. Polysaccharide film preparation

Chitosan from crab shells (minimum 85% deacetylated) and 11-mercapto-1-undecanol (97%) were purchased from Sigma–Aldrich Chemicals, amylose (soluble starch) from E.Merck. The gold substrates (200 nm Au on Si wafer) were purchased from Georg Albert PVD-Coating. The gold substrates were pre-coated with a SAM of 11-mercapto-1-undecanol by immersion into an ethanolic solution for 24 h, followed by thorough rinsing with ethanol and drying. Chitosan solution (0.5%, v/w) was prepared by immersion of chitosan flakes in water and addition of small amounts of HCl to the solution to adjust the pH to 3. After stirring for 4 h, the chitosan solution was filtered and the pH was adjusted to 5.5 using NaOH. Amylose solution (0.5%, v/w) was prepared by adding the powder to water, stirring and subsequent heating to the boiling point. Chitosan and amylose films were prepared on the pre-coated Au substrates by spin-coating (3000 rpm, 90 s). After spin-coating, the amylose films were dried at 100 °C for 2 h, the chitosan films were dried at room temperature for approximately 12 h. The thickness of the films studied in RAIRS was approximately 40 nm according to ellipsometry. Films used for XPS experiments had an average thickness of 7 nm as determined from the attenuation of the Au 4f signal.

2.2. Electron exposure

Electron exposure of samples used to investigate the wetting properties and for RAIRS was performed in a high-vacuum chamber equipped with a commercial non-monochromatized electron flood gun (SPECS FG 15/40) after the base pressure had reached a 10^{-8} Torr range. The electron energy (E_0) was set at nominal values ranging from 5 eV to 15 eV. Following exposure, the chamber was vented by backfilling with N_2 and the samples were quickly transferred under ambient conditions to the RAIRS setup. As pronounced changes in wetting properties and in RAIR spectra were already observed at the lowest investigated E_0, additional XPS experiments were performed on samples before and after exposure at E_0 = 5.2 eV. Electron exposure in these experiments was performed in situ using the electron gun of an Omicron LEED instrument. Electron exposure during HREELS experiments was also performed in situ again using the FG 15/40 flood gun.

2.3. Reflection absorption infrared spectroscopy

RAIR spectra (400 scans each) were acquired under vacuum at a resolution of 4 cm^{-1} using a Bruker IFS 66v/S spectrometer after removal of the samples from the high-vacuum chamber. Control experiments were performed with samples that were equally stored in vacuum but not exposed. Decomposition was not observed in this case.

2.4. X-ray photoelectron spectroscopy

XPS data were acquired in an Omicron UHV setup using Mg K_α radiation and a Leybold electron energy analyser. The peak positions were corrected for possible charging effects by referring to the signal of the underlying Au substrate (4f doublet at 84.1 eV and 87.7 eV). XPS as function of electron exposure was measured on two specific samples for both amylose and chitosan.

2.5. High-resolution electron energy loss spectroscopy

HREELS experiments were performed using a μ-metal-shielded UHV chamber reaching a base pressure of 10^{-10} mbar and connected to a sample preparation chamber with a base pressure of about 2×10^{-9} mbar (Swiderek & Winterling, 1998). In the latter chamber, α-D-glucose (Acros Organics, ≥99%, named glucose hereafter) was deposited from the vapour phase onto a polycrystalline Pt substrate using a heatable quartz glass as evaporation source. The evaporator is introduced via a load lock chamber equipped with XYZ manipulator. A quartz crystal microbalance (QMB) positioned in front of the evaporator inside the load lock system is used to measure the sample deposition rate at room temperature. After establishing a constant deposition rate by mild heating (a few 10 °C) the source was transferred into the preparation chamber and positioned in front of the Pt substrate which was cooled using a closed-cycle He cryostat (Leybold) and cleaned by resistive heating prior to deposition. Sample and QMB were positioned at the same distance from the source. Glucose was deposited upon maintaining the Pt substrate between 25 K and 30 K as estimated from the condensation behaviour of O_2 and CO gas. The deposition rate measured at room temperature thus yields a lower limit for the actual deposition rate on the cold Pt substrate.

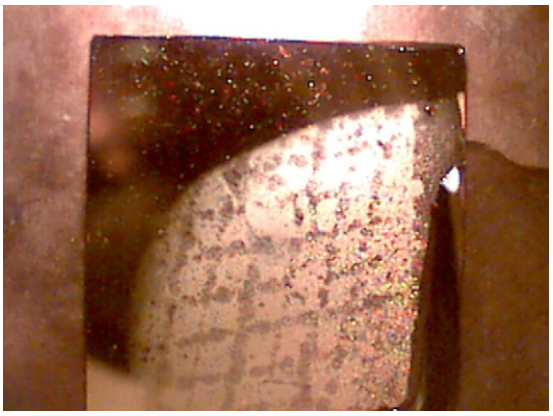

Fig. 2. Condensation of water vapour on a gold substrate spin-coated with an amylose film after an exposure of 8000 μC (2000 μC/cm^2) to electrons with incident energy of 15 eV. The substrate was partially covered by a metal grid during irradiation.

Electron exposure was also performed in the sample preparation chamber. For exposure in the presence of O_2, the gas (Air Liquide, 99.998 vol.%) was leaked into the preparation chamber via a tube ending in the vicinity of the substrate to reach a background pressure of 2.5×10^{-8} Torr. The pressure near the sample consequently must have been higher but has not been determined here.

For data acquisition the cryostat was transferred to the HREEL chamber. Spectra were acquired at an incident electron energy (E_0) of 5.5 eV using an instrument consisting of a rotatable cylindrical double pass monochromator set to 56° with respect to the normal of the sample and a single pass electron energy analyser fixed at 60° at the opposite azimuth. The resolution was 12–15 meV (FWHM of the elastic peak) for currents of 0.2–0.3 nA as measured on the Pt substrate. E_0 was calibrated as described previously (Swiderek & Winterling, 1998).

3. Results

3.1. Modification of amylose films by low-energy electron exposure

3.1.1. Wetting properties

The change in surface properties of amylose films due to electron exposure was investigated by observing their wetting behaviour. The samples were covered by a grid and then exposed to electrons at E_0 = 5 eV, 10 eV, and 15 eV. Afterwards, the samples were exposed to water vapour so that water condensed on the surface. The formation of droplets occurred preferentially on the area that was covered by the grid. This is shown in Fig. 2 for E_0 = 15 eV and an exposure of 2000 μC/cm^2. The effect was less pronounced but still visible at lower E_0. The result suggests that the exposed areas become hydrophobic during electron exposure so that formation of a first water layer that is necessary for further condensation is less likely. Consequently, more water can condense and coalesce to larger droplets in the non-exposed surface areas. Electron exposure thus can serve to modify the surface properties of amylose coatings in order to make them water-repellent.

3.1.2. XPS

XPS data for thin films of amylose are presented in Fig. 3. The O1s signal consists of a single band with maximum at 532.5 eV which is characteristic of alcohols (Amaral, Granja, & Barbosa, 2005; Wagner et al., 2003). This band decreases under electron exposure pointing towards loss of oxygen. C1s spectra show an unresolved peak with two components centred at approximately 285 eV (saturated CH_2 group; Amaral et al., 2005; Wagner et al., 2003) and 286.4 eV (C adjacent to OH; Wagner et al., 2003). A further small shoulder is located around 288 eV and can be ascribed to C1 (O–C–O unit; Amaral et al., 2005). Upon electron exposure at E_0 = 5.2 eV, the latter two signals decrease and a single strong signal at 285 eV is formed. These results show that electron exposure at E_0 as low as 5.2 eV leads to loss of O and consequently to the formation of a hydrocarbon material with low oxygen content.

3.1.3. RAIRS

RAIR spectra of the spin-coated amylose films (Fig. 4) show a characteristic band system between 950 cm^{-1} and 1200 cm^{-1} that closely reproduces previous infrared results obtained by both transmission (Cael, Koenig, & Blackwell, 1975; Nikonenko, Buslov, Sushko, & Zhbankov, 2005) and DRIFT spectroscopy (Smits, Ruhnau, Vliegenthart, & van Soest, 1998). Other signals are weak or uncharacteristic and are thus not shown here. All of the bands with pronounced maxima at 1155 cm^{-1}, 1083 cm^{-1}, and 1049 cm^{-1} relate to the C–O and C–C stretching vibrations with contributions from COH bending (Cael et al., 1975). Furthermore, it has been suggested that the glycosidic C–O–C bridges contribute particularly to the highest frequency signal and to the intensity between 1000 cm^{-1} and 920 cm^{-1} (Nikonenko et al., 2005) and that the exact position of the lowest band depends on the degree of order within the sample (1047 cm^{-1} for a more organized solid, 1022 cm^{-1} for amorphous amylose; Smits et al., 1998). The slight differences in band shape for the lowest maximum in the case of the two samples shown in Fig. 4 are thus ascribed to a different degree of order within the spin-coated films.

Electron exposure of the amylose films at E_0 = 5 eV leads to a general decrease of the band intensities that becomes more pronounced with increasing exposure (Fig. 4). The strong loss of intensity in the RAIR spectra thus points to a considerable loss of C–O bonds in the amylose films due to electron exposure consistent with the XPS results. After 1000 μC, an additional weak signal is visible at 1726 cm^{-1} with a small sideband at 1760 cm^{-1}. This band can be assigned to carboxylic acid groups (Conley, 1966) that were also observed previously in polysaccharides following high-energy radiation treatment (Sharpatyi, 2003). At higher exposure, these products, or their precursors, assuming that the carboxylic

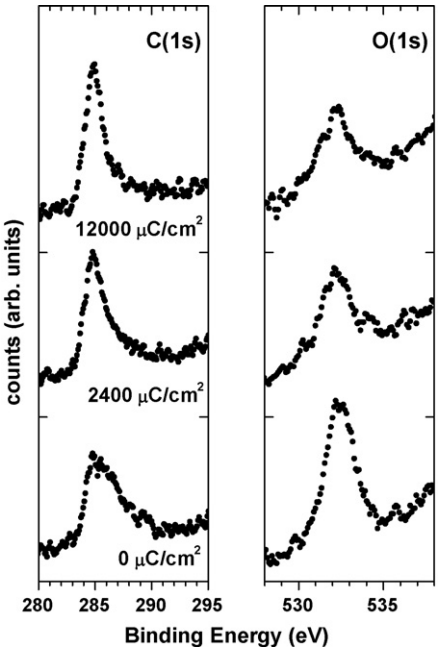

Fig. 3. XPS spectra of a gold substrate spin-coated with an amylose film before and after the stated exposures to electrons with incident energy of 5.2 eV.

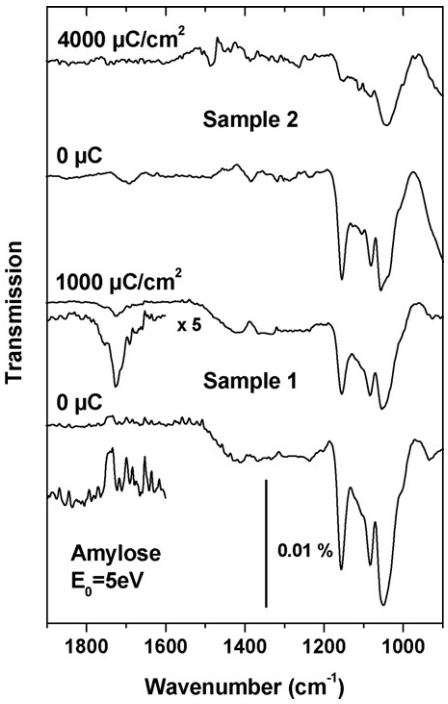

Fig. 4. RAIR spectra of two representative gold substrates spin-coated with amylose films before and after the stated exposures to electrons with incident energy of 5 eV.

acid groups are formed by reaction of initial reactive fragments with air after removal of the sample from the irradiation chamber, are equally decomposed so that the corresponding bands are not discernible. Irradiation at E_0 = 15 eV leads to a very similar loss of intensity of the C–O stretching band system (not shown) pointing towards a comparable decomposition of the amylose film.

3.2. Modification of chitosan films by low-energy electron exposure

3.2.1. Wetting properties

In the case of chitosan samples a pronounced change in wetting properties analogous to the amylose samples could not be observed. The reason for this pronounced difference is investigated in the following sections.

3.2.2. XPS

XPS data for thin films of chitosan are presented in Fig. 5. The O1s signals of the OH groups (532.9 eV), the ether linkage (533.5 eV), and the amide group (531.6 eV) (Amaral et al., 2005) appear as one single peak at the resolution of the present XPS experiment. Again, an overall decrease of the O1s signal is observed upon electron exposure. The C1s signal displays three contributions centred at 285 eV and assigned to $-CH_2-$ or $C-NH_2$ (Amaral et al., 2005), at 286.4 eV (C adjacent to OH (Wagner et al., 2003) or C adjacent to the amide group (Amaral et al., 2005)), and 288.3 eV (O–C–O or –C=O; Amaral et al., 2005). Again, the signals at higher binding energy decrease upon exposure but to a lower extent than observed for amylose. Unfortunately, due to overlap of the signals ascribed to the sugar ring and the amide side group, this result alone does not allow us to distinguish which part of the molecule is more strongly affected by electron exposure. Finally, the N1s signal near 400 eV is weak and does not change noticeably.

The incomplete decay of the C1s signal components at higher binding energy shows that the loss of oxygen under electron exposure at E_0 = 5.2 eV is less pronounced in chitosan than in amylose. The presence of the amide group thus modifies the electron-induced reactivity. The constant N1s intensity, on the other hand, suggests that nitrogen is not removed from the sugar to an important extent under electron exposure.

3.2.3. RAIRS

The RAIR spectra of chitosan films prior to electron exposure are shown in Fig. 6. The observed band positions as well as previous infrared data are summarized in Table 1. The various C–O and C–C stretching vibrations again appear between 1000 cm^{-1} and 1200 cm^{-1} but are less clearly resolved than in amylose due to small spacing between several bands of similar intensity (Amaral et al., 2005; Brugnerotto et al., 2001; Lawrie et al., 2007; López-Pérez, Marques, da Silva, Pashkuleva, & Reis, 2007). Consequently, the reported position of the band maximum varies. Amide bands are present because the deacetylation of the commercial chitosan is usually incomplete. Table 1 thus includes reference data for both chitosan and chitin. The present RAIR spectra of non-exposed chitosan films reproduce well the previous infrared data except for the amide II band at 1522 cm^{-1}. This effect can be traced back to the fact that the present films were produced from an acidic solution as supported by frequencies between 1520 cm^{-1} and 1530 cm^{-1} observed previously for films cast from hydrochloric or lactic acid solutions (Lawrie et al., 2007).

Exposure of the chitosan films to electrons at E_0 = 5 eV leads to a rapid loss of intensity of the amide bands, an increase of a band around 1455 cm^{-1} ascribed to CH_2 or CH_3 deformation modes and again the appearance of carboxylic acid signals at 1730 cm^{-1} (Fig. 6). The 1522 cm^{-1} band shows the most rapid decrease, in accord with its assignment as the vibration of a protonated amino group that must have a high affinity to electrons due to its positive charge. Contrary to amylose, the C–O stretching vibrations do not decrease. Chitosan thus appears to be less sensitive regarding loss of oxygen under exposure to low-energy electrons than amylose. The nature of the remaining nitrogen deduced from XPS is not immediately obvious from the RAIR spectra. However, the deacetylated amino groups present in chitosan can contribute to the remaining intensity of the C=O stretching band (maximum 1658 cm^{-1}) and cause its asymmetry towards lower wavenumbers (Conley, 1966). In summary, the RAIR spectra point towards a rapid degradation

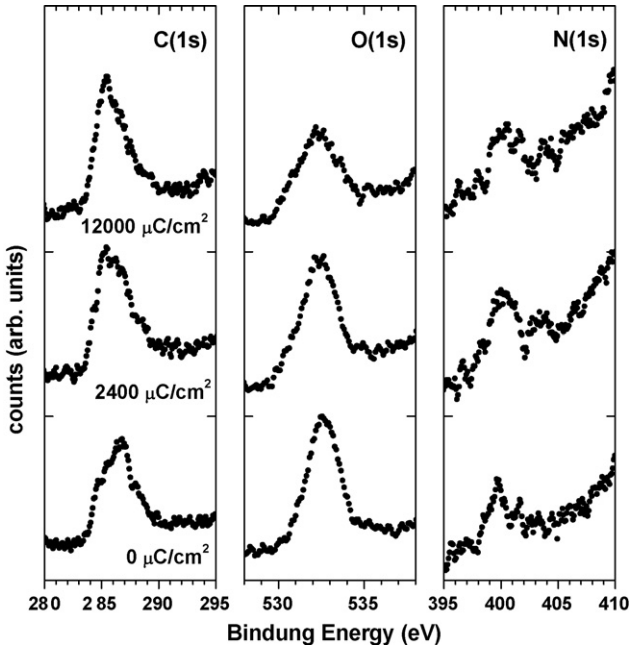

Fig. 5. XPS spectra of a gold substrate spin-coated with a chitosan film before and after the stated exposures to electrons with incident energy of 5.2 eV.

Table 1
Comparison of RAIRS signals of spin-coated chitosan films with previous infrared spectroscopic data.

Band position [cm^{-1}]		Assignment	Reference
This work	Previous work		
1658	1650	–C=O stretch (amide I) in chitosan amide I in chitosan	Amaral et al. (2005)
	1645		Lawrie et al. (2007)
	1656	–C=O stretch (amide I), single H-bonded to NH in chitin	Yamaguchi, Nge, Takemura, Hori, and Ono (2005)
1630	1622	–C=O stretch (amide I), double H-bonded to NH and CH_2OH in chitin	Yamaguchi et al. (2005)
1522	1558	N–H in plane deformation coupled with C–N stretching (amide II) in chitosan	Amaral et al. (2005)
	1584	N–H bending from amine and amide II in chitosan	Lawrie et al. (2007)
	1560	Amide II in chitin	Yamaguchi et al. (2005)
1410	1414	CH_2 bending	Lawrie et al. (2007)
1377	1375	CH_3 symmetric deformation	Amaral et al. (2005) and Lawrie et al. (2007)
1320	1317, 1324	CH_2 wagging coupled with OH; C–N stretch coupled with NH in plane deformation (amide III)	Amaral et al. (2005) and López-Pérez et al. (2007)
1262			
1150 (sh)	1150	Antisymmetric C–O–C stretching (glycosidic linkage) and C–N stretch	Lawrie et al. (2007) and López-Pérez et al. (2007)
1080	Max variable	Skeletal vibrations of C–O stretching	Amaral et al. (2005), Lawrie et al. (2007), López-Pérez et al. (2007) and Brugnerotto et al. (2001)

of the amide groups under low-energy electron exposure while the OH groups of the sugar are less affected than in the case of amylose.

3.3. *Effect of O_2 on reactions induced by low-energy electron exposure*

Electron exposure in the XPS experiments was performed in situ, i.e., under UHV, while samples used in RAIRS experiments were irradiated in high vacuum and handled under ambient conditions afterwards. This raises questions about the effect of contact with reactive atmospheric constituents, the most important being O_2. Both the XPS setup and the irradiation chamber used in this work were not equipped for dosing gases during electron exposure. This, on the other hand, was possible in a separate setup dedicated to HREELS. HREEL spectra of amylose and chitosan films could not successfully be recorded due to the low conductivity of the spin-coated films. Already a slight build-up of charge, that would not affect irradiation by a defocused electron beam, can severely disturb the focused low-energy and low-current beam from the HREEL spectrometer and thus disable this measurement. Therefore, thin layers of α-D-glucose as a model monomer were produced by deposition from the vapour and their modification during electron exposure was monitored.

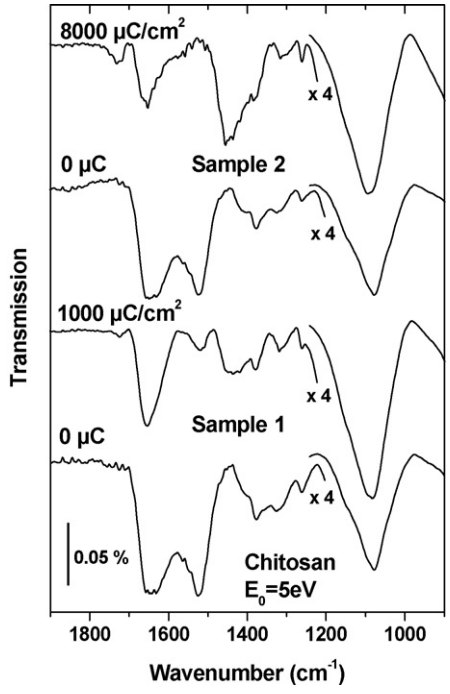

Fig. 6. RAIR spectra of two representative gold substrates spin-coated with chitosan films before and after the stated exposures to electrons with incident energy of 5 eV.

The HREEL spectrum of non-exposed glucose (Fig. 7, bottom) has been assigned by comparison with vibrational frequencies from infrared and Raman experiments (Ibrahim, Alaam, El-Haes, Jalbout, & de Leon, 2006; Vasko, Blackwell, & Koenig, 1972) and both DFT calculations (Vasko et al., 1972) and normal coordinate analysis (Ibrahim et al., 2006). The dominant are the C–O stretching modes (136 meV), a combination of OCH, COH, and CCH angle deformation vibrations (170 meV), and the C–H (362 eV) and O–H (400–460 meV) stretching vibrations. Minor signals at 42 meV and 71 meV most likely relate to torsional motions and ring deformations (Vasko et al., 1972) while small bands at 270 meV, 308 meV, and 498 meV can be ascribed to multiple scattering bands. The O–H stretching band is broad pointing towards extensive hydrogen bonding in the glucose film but includes a more pronounced maximum centred around 444 meV. Based on the results of matrix-isolation study (Krasnokutski et al., 1998), the maximum at 444 meV is assigned to O–H vibrations of intramolecularly hydrogen-bonded O–H groups while the broad band extending down to 400 meV is ascribed to stronger intermolecular hydrogen bonds.

Electron exposure at $E_0 = 5$ eV of thin films of glucose under UHV conditions leads to characteristic changes in the HREEL spectra (Fig. 7, middle). Most importantly, the intensity distribution within the O–H stretching band changes such that the characteristic peak at 444 meV vanishes rapidly and the maximum of the remaining band shifts to lower energy losses. This indicates that weakly hydrogen-bonded OH groups are preferentially lost under electron exposure. A loss of OH groups is in accord with the XPS and RAIRS results on amylose. The important intensity in the range of CH stretching vibrations again indicates that a hydrocarbon material remains after electron exposure.

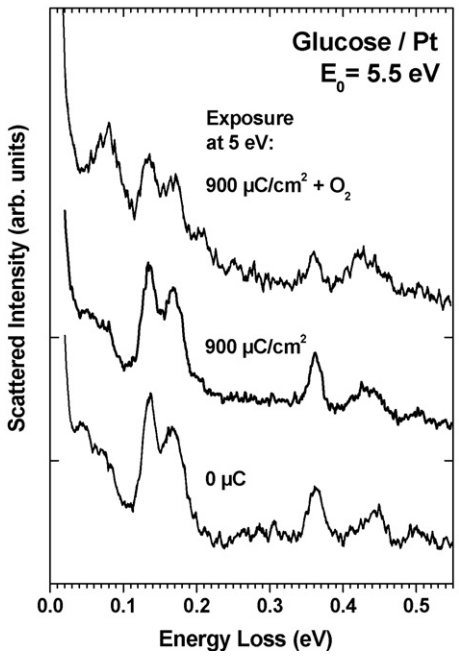

Fig. 7. HREEL spectra of a freshly deposited film of α-D-glucose (bottom) and spectrum of the same film after electron exposure of 4000 μC at E_0 = 5 eV in the presence of O_2 (top). For comparison, the spectrum of an equivalent film after electron exposure of 4000 μC at E_0 = 5 eV without the presence of O_2 is included (middle). According to the room temperature quartz microbalance measurement a lower limit to the thickness of the films can be stated as monolayer coverage.

The outcome of the electron-induced reactions is noticeably different when O_2 is present (Fig. 7, top). In this case, an intense new band appears at 82 meV. This band is characteristic of the formation of CO_2 and relates to the CO_2 bending vibration (Bertin et al., 2009). In HREEL spectra of CO_2 recorded under comparable conditions, the corresponding CO stretching band has been observed previously at 291 meV but with relatively low intensity (Bertin et al., 2009). This band is consequently difficult to detect in the present experiment. As another change due to electron exposure, the relative intensity of the CH stretching band decreases. Finally, a new signal appears at 205 meV. This is tentatively assigned to the bending mode of H_2O. A CC double bond stretching band would appear in the same energy loss range but should be accompanied by a broadening of the CH stretching peak towards higher energy loss. This possibility is thus excluded here. Together, the results point towards a rapid degradation of glucose including the carbon contents under electron exposure in the presence of O_2.

It must be noted that O_2 neither condenses on nor changes the sample under the present experimental conditions as verified in a blind experiment without electron exposure. In the exposure experiment, O_2 was thus either dissociated by electron impact above the sample surface and the produced fragments collided with the surface to initiate subsequent reactions or O_2 was adsorbed shortly at the surface and dissociated by the impinging electrons in the immediate vicinity of the condensed glucose. Nonetheless, the formation of CO_2 and intensity decrease of the CH stretching band implies that electron exposure in the presence of O_2 induces a considerable oxidation of glucose.

4. Discussion

Recent investigations of the modification of polysaccharides by high-energy radiation have identified products, determined their yields and consequently proposed mechanisms of the inherent chemical changes to the materials (Huang et al., 2007; Kabanov et al., 2009; Korotchenko, Pristupa, & Sharpatyi, 2004; Sharpatyi, 2003). The high-radiation chemistry clearly relates to the low-energy electron-induced processes investigated in the present work as discussed in this section.

The present results provide the first evidence that polysaccharides are efficiently modified or decomposed by exposure to low-energy electrons. Different electron–molecule interaction mechanisms can be held responsible for inducing chemical reactions under the effect of an electron beam (Arumainayagam, Lee, Nelson, & Haines, 2010; Bald, Langer, Tegeder, & Ingólfsson, 2008; Illenberger & Momigny, 1992). For E_0 above the ionisation threshold, an electron is ejected from the molecule, often leading to subsequent fragmentation:

$$AB + e^- \rightarrow AB^+ + 2e^- \quad (1a)$$

$$AB^+ \rightarrow A + B^+ \quad (1b)$$

Alternatively, and as most efficient reaction channel below the ionisation threshold, an electron can temporarily be trapped by the molecule to form a short-lived negative ion which subsequently can again decay by fragmentation:

$$AB + e^- \rightarrow AB^{*-} \rightarrow A + B^- \quad (2)$$

This so-called dissociative electron attachment (DEA) occurs within relatively narrow ranges of E_0, depending on the specific electronic state of AB^{*-}. Different states of AB^{*-} (resonances) typically decay via different fragmentation routes. An excellent example is DEA to the nucleobase thymine where each H atom can be selectively abstracted by tuning E_0 to appropriate values (Swiderek, 2006).

The reactions for amylose are most likely related to DEA processes observed with a threshold of 5 eV in monomeric gaseous sugars (Baccarelli et al., 2007; Bald et al., 2006; Ptasińska et al., 2004; Sulzer et al., 2006) with fructose (Sulzer et al., 2006) being the most similar to the amylose monomer glucose. Expulsion of O^- from a C–O–H unit by DEA is a prominent process just above this threshold. It is energetically accessible due to simultaneous formation of a new C–H bond (Sulzer et al., 2006). This process can explain the decrease of the C–O stretching band intensity in the RAIR spectra of amylose films under low-energy electron exposure and the formation of a hydrocarbon material as observed in XPS. However, it is at first sight surprising that the reactions in polysaccharide films are fairly efficient already at E_0 corresponding to the threshold of fragmentation via DEA as observed in the gas phase. Two effects must be considered here. First, the energy of an ionic state in the condensed phase is typically lowered by 1–2 eV as compared to the gas phase (Pope & Swenberg, 1999). This stabilisation is due to the polarisation of the surrounding medium by the ion and the resulting attractive interaction. Second, the electron gun delivers a non-monochromatic electron beam, i.e., the electrons have an energy distribution with width of approximately 0.5–1 eV. The E_0 dependence of a reactive process convoluted with the E_0 distribution of the gun yields the apparent E_0 dependence. Both the polarisation stabilisation of the initial ionic fragments within the solid phase and the large energy distribution of the electron gun used in the present experiments will lead to a decrease of the onset in the apparent E_0 dependence of a DEA process and can thus explain the obvious efficiency of the reaction in solid amylose films at E_0 as low as 5 eV.

The formation of carboxyl groups suggested by the present RAIR spectra for both amylose and chitosan has not been described in the previous low-energy exposure studies of gaseous saccharide monomers (Baccarelli et al., 2007; Bald et al., 2006; Ptasińska et al., 2004; Sulzer et al., 2006). This is partly explained by the fact that only mass spectrometry but not vibrational spectroscopy was applied. Recent high-energy radiation work on polysaccharides has

detected different carboxylic acids as products of exposure (Huang et al., 2007; Korotchenko et al., 2004). However, the presence of oxygen is necessary to explain such products in polysaccharides (Korotchenko et al., 2004; Sharpatyi, 2003). Irradiation alone can produce acids only in saccharide monomers where the C1 carbon is not involved in a glycosidic bond (Abagyan & Apresyan, 2002). Therefore, carboxyl groups may result from residual air present in the high-vacuum chamber during irradiation of the samples used for RAIRS experiments or radical sites that are produced in the material during exposure and react with atmospheric oxygen upon transfer from the irradiation chamber to the RAIRS setup. This is also suggested by the present results from HREEL spectroscopy which show that electron exposure induces the well-known oxidation of the sugar to CO_2 already at cryogenic temperatures where an activation barrier otherwise prevents the reaction from taking place. While a relatively high O_2 partial pressure was applied here, this result suggests that a lower partial pressure of O_2 as present in the case of a residual gas can lead to partial oxidation of the saccharide thus rationalising the observation of carboxylic acid groups in RAIRS. In this model experiment, it can, however, not be ruled out that reactive sites produced by electron exposure in situ are long-lived enough to react with O_2 either in situ or later upon contact with ambient air.

The effect of low-energy electrons on saccharides with side groups other than OH has not been studied so far. However, high-energy studies have shown that chitin and chitosan are considerably more resistant to radiation than starch (Kabanov et al., 2009). This effect was traced back to a protective action of the amide and amino side groups that would be more prone to excitation than the rest of the molecular units. This finding is consistent with the results obtained here, namely the more pronounced reactivity of the amide group in chitosan as compared to the OH groups. Recent experiments on acetamide have revealed a high reactivity towards low-energy electrons leading to severe fragmentation of the molecule (Koenig-Lehmann, Kopyra, Dąbkowska, Kočišek, & Illenberger, 2008). Unfortunately, cross-sections for this process were not reported. However, cross-sections for decomposition of a carbonyl-containing structure, namely acetaldehyde, have been reported near 5×10^{-17} cm^2 for $E_0 = 6$ eV (Burean & Swiderek, 2008). NH_3 as a model for an amino group, on the other hand, undergoes decomposition via DEA with a total cross-sections of 3.9×10^{-18} cm^2 at 5.7 eV (Rawat, Prabhudesai, Rahman, Barghava Ram, & Krishnakumar, 2008). This suggests at least that amino groups may react considerably slower than amide groups under low-energy electron exposure and consequently support the proposed assignment of the remaining nitrogen observed in XPS to amino groups of the chitosan. Similarly, the finding that the amide groups in chitosan are decomposed more rapidly under exposure to low-energy electrons than the OH groups is reminiscent of the previous result that cross-sections for formation of CO in methanol (Lepage, Michaud, & Sanche, 1997) is more than an order of magnitude smaller than in acetone (Lepage, Michaud, & Sanche, 2000). Carboxyl groups thus have a particularly high reactivity as compared to OH groups under exposure to low-energy electrons.

5. Conclusions

The effect of low-energy electron irradiation on thin polysaccharide films has been investigated for the first time. Electron exposure leads to a significant modification of the wetting properties of amylose films. This change can be traced back to a loss of oxygen leading to formation of a hydrocarbon material. In contrast, the amide groups are most rapidly decomposed in exposed chitosan while the loss of hydroxyl groups is less severe than in amylose. The results equally demonstrate that the reactivity of the polysaccharide is controlled by the presence of side groups that react faster under the electron beam than the sugar itself. These groups protect the polysaccharide backbone from immediate decomposition. The presence of oxygen during electron exposure leads to oxidation of the saccharide as demonstrated for the example of glucose.

Acknowledgements

Support provided by the Cost Action CM0601 “Electron Controlled Chemical Lithography” (ECCL) and the ESF program “Electron Induced Processes At the Molecular Level” (EIPAM) is gratefully acknowledged.

References

Abagyan, G. V., & Apresyan, A. S. (2002). Reaction routes of free radicals in γ-irradiated α-D-glucose. *High Energy Chemistry*, *36*, 229–235.
Amaral, I. F., Granja, P. L., & Barbosa, M. A. (2005). Chemical modification of chitosan by phosphorylation: An XPS, FT-IR and SEM study. *Journal of Biomaterial Science, Polymer Edition*, *16*, 1575–1593.
Arumainayagam, C. R., Lee, H.-L., Nelson, R. B., & Haines, D. R. (2010). Low-energy electron-induced reactions in condensed matter. *Surface Science Reports*, *65*, 1–44.
Baccarelli, I., Gianturco, F. A., Grandi, A., Sanna, N., Lucchese, R. R., Bald, I., et al. (2007). Selective bond breaking in β-D-ribose by gas-phase electron attachment around 8 eV. *Journal of the American Chemical Society*, *129*, 6269–6277.
Bald, I., Kopyra, J., & Illenberger, E. (2006). Selective excision of C5 from D-ribose in the gas phase by low-energy electrons (0–1 eV): Implications for the mechanism of DNA damage. *Angewandte Chemie International Edition*, *45*, 4851–4855.
Bald, I., Langer, J., Tegeder, P., & Ingólfsson, O. (2008). From isolated molecules through clusters and condensates to the building blocks of life: A short tribute to Prof. Eugen Illenberger's work in the field of negative ion chemistry. *International Journal of Mass Spectrometry*, *277*, 4–25.
Bertin, M., Martin, I., Duvernay, F., Theule, P., Bossa, J. B., Borget, F., et al. (2009). *Physical Chemistry Chemical Physics*, *11*, 1838–1845.
Brugnerotto, J., Lizardi, J., Goycoolea, F. M., Argüelles-Monal, W., Desbrières, J., & Rinaudo, M. (2001). An infrared investigation in relation with chitin and chitosan characterization. *Polymer*, *42*, 3569–3580.
Burean, E., & Swiderek, P. (2008). Electron-induced reactions in condensed acetaldehyde: Identification of products and energy-dependent cross sections. *Journal of Physical Chemistry C*, *112*, 19456–19464.
Cael, J. J., Koenig, J. L., & Blackwell, J. (1975). Infrared and Raman spectroscopy of carbohydrates. Part VI: Normal coordinate analysis of V-amylose. *Biopolymers*, *14*, 1885–1903.
Conley, R. T. (1966). *Infrared spectroscopy*. Boston: Allyn and Bacon.
Eck, W., Stadler, V., Geyer, W., Zharnikov, M., Gölzhäuser, A., & Grunze, M. (2000). Generation of surface amino groups on aromatic self-assembled monolayers by low energy electron beams—A first step towards chemical lithography. *Advanced Materials*, *12*, 805–808.
Hai, L., Diep, T. B., Nagasawa, N., Yoshii, F., & Kume, T. (2003). Radiation depolymerization of chitosan to prepare oligomers. *Nuclear Instruments and Methods in Physics Research B*, *208*, 466–470.
Huang, L., Peng, J., Zhai, M., Li, J., & Wie, G. (2007). Radiation-induced changes in carboxymethylated chitosan. *Radiation Physics and Chemistry*, *76*, 1679–1683.
Ibrahim, M., Alaam, M., El-Haes, H., Jalbout, A. F., & de Leon, A. (2006). Analysis of the structure and vibrational spectra of glucose and fructose. *Eclética Química (São Paulo)*, *31*, 15–21.
Illenberger, E., & Momigny, J. (1992). *Gaseous molecular ions. An introduction to elementary processes induced by ionization*. New York: Springer.
Kabanov, V. Ya., Feldman, V. I., Ershov, B. G., Polikarpov, A. I., Kiryukhin, D. P., & Apel, P. Yu. (2009). Radiation chemistry of polymers. *High Energy Chemistry*, *43*, 1–18.
Khan, F., Ahmad, S. R., & Kronfli, E. (2006). γ-Radiation induced changes in the physical and chemical properties of lignocellulose. *Biomacromolecules*, *7*, 2303–2309.
Koenig-Lehmann, C., Kopyra, J., Dąbkowska, I., Kočišek, J., & Illenberger, E. (2008). Excision of CN– and OCN– from acetamide and some amide derivatives triggered by low energy electrons. *Physical Chemistry Chemical Physics*, *10*, 6954–6961.
Korotchenko, K. A., Pristupa, A. I., & Sharpatyi, V. A. (2004). Radiation chemistry of polysaccharides: 2. Free-radical mechanisms of formation of citric acid and dicarboxylic acids. *High Energy Chemistry*, *38*, 81–85.
Krasnokutski, S. A., Ivanov, A., Izvekov, Yu., Sheina, V., Blagoi, G. G., & Yu, P. (1998). FTIR matrix isolation study of uridine, thymidine, ribose, and glucose. *Journal of Molecular Structure*, *482–483*, 249–252.
Lawrie, G., Keen, I., Drew, B., Chandler-Temple, A., Rintoul, L., Fredericks, P., et al. (2007). Interactions between alginate and chitosan biopolymers characterized using FTIR and XPS. *Biomacromolecules*, *8*, 2533–2541.
Lepage, M., Michaud, M., & Sanche, L. (1997). Low energy electron total scattering cross section for the production of CO within condensed methanol. *Journal of Chemical Physics*, *107*, 3478–3484.
Lepage, M., Michaud, M., & Sanche, L. (2000). Low energy electron scattering cross section for the production of CO within condensed methanol. *Journal of Chemical Physics*, *113*, 3602–3608.

Long, D., Wu, G., & Chen, S. (2007). Preparation of oligochitosan stabilized silver nanoparticles by gamma irradiation. *Radiation Physics and Chemistry*, *76*, 1126–1131.

López-Pérez, P. M., Marques, A. P., da Silva, R. M. P., Pashkuleva, I., & Reis, R. L. (2007). Effect of chitosan membrane surface modification via plasma induced polymerization on the adhesion of osteoblast-like cells. *Journal of Materials Chemistry*, *17*, 4064–4071.

Nikonenko, N. A., Buslov, D. K., Sushko, N. I., & Zhbankov, R. G. (2005). Spectrosopic manifestation of stretching vibration of glycosidic linkage in polysaccharides. *Journal of Molecular Structure*, *752*, 20–24.

Pekel, N., Yoshii, F., Fume, T., & Güven, O. (2004). Radiation crosslinking of biodegradable hydroxypropylmethylcellulose. *Carbohydrate Polymers*, *55*, 139–147.

Pope, M., & Swenberg, C. E. (1999). *Electronic processes in organic crystals and polymers*. Oxford: Oxford University Press.

Ptasińska, S., Denifl, S., Scheier, P., & Märk, T. D. (2004). Inelastic electron interaction (attachment/ionization) with deoxyribose. *Journal of Chemical Physics*, *120*, 8505–8511.

Rawat, P., Prabhudesai, V. S., Rahman, M. A., Barghava Ram, M., & Krishnakumar, E. (2008). Absolute cross sections for dissociative electron attachment to NH_3 and CH_4. *International Journal of Mass Spectrometry*, *277*, 96–102.

Sharpatyi, V. A. (2003). Radiation chemistry of polysaccharides: 1. Mechanisms of carbon monoxide and formic acid formation. *High Energy Chemistry*, *37*, 369–372.

Sim, K. S., & White, J. D. (2005). New technique for *in situ* measurement of backscattered and secondary electron yields for the calculation of signal-to-noise ratio in a SEM. *Journal of Microscopy*, *217*, 235–240.

Smits, A. L. M., Ruhnau, F. C., Vliegenthart, J. F. G., & van Soest, J. J. G. (1998). Aging of starch based systems as observed with FT-IR and solid state NMR spectroscopy. *Starch/Stärke*, *50*, 478–483.

Sulzer, P., Ptasińska, S., Zappa, F., Mielewska, B., Milosavljevic, A. R., Scheier, P., et al. (2006). Dissociative electron attachment to furan, tetrahydrofuran, and fructose. *Journal of Chemical Physics*, *125*, 044304.

Swiderek, P. (2006). Fundamental processes in radiation damage of DNA. *Angewandte Chemie International Edition*, *45*, 4056–4059.

Swiderek, P., & Winterling, H. (1998). Spin-forbidden transitions in amorphous and crystalline thin films of benzene. *Chemical Physics*, *229*, 295–307.

Vasko, P. D., Blackwell, J., & Koenig, J. L. (1972). Infrared and Raman spectroscopy of carbohydrates. Part II: Normal coordinate analysis of a-D-glucose. *Carbohydrate Research*, *23*, 407–416.

Wagner, C. D., Naumkin, A. V., Kraut-Vass, A., Allison, J. W., Powell, C. J., & Rumble, J. R., Jr. (2003). *NIST X-ray photoelectron spectroscopy database, NIST standard reference database 20, version 3.5*. http://srdata.nist.gov/xps/Default.aspx

Wu, L.-Q., Lee, K., Wang, X., English, D. S., Losert, W., & Payne, G. F. (2005). Chitosan-mediated and spatially selective electrodeposition of nanoscale particles. *Langmuir*, *21*, 3641–3646.

Yamaguchi, Y., Nge, T. T., Takemura, A., Hori, N., & Ono, H. (2005). Characterization of uniaxially aligned chitin film by 2D FT-IR spectroscopy. *Biomacromolecules*, *6*, 1941–1947.

Yoshii, F., Zhao, L., Wach, R. A., Nagasawa, N., Mitomo, H., & Kume, T. (2003). Hydrogels of polysaccharide derivatives crosslinked with irradiation at paste-like condition. *Nuclear Instruments and Methods in Physics Research B*, *208*, 320–324.

Zhai, M., Yoshii, F., & Fume, T. (2003). Radiation modification of starch-based plastic sheets. *Carbohydrate Polymers*, *52*, 311–317.

Zhao, L., Mitomo, H., Zhai, M., Yoshii, F., Nagasawa, N., & Kume, T. (2003). Synthesis of antibacterial PVA/CM-chitosan blend hydrogels with electron beam irradiation. *Carbohydrate Polymers*, *53*, 439–446.